Quality control and assurance in functional near infrared spectroscopy (fNIRS) experimentation

To cite this article: F Orihuela-Espina *et al* 2010 *Phys. Med. Biol.* **55** 3701

IOP PUBLISHING PHYSICS IN MEDICINE AND BIOLOGY

Phys. Med. Biol. **55** (2010) 3701–3724 doi:10.1088/0031-9155/55/13/009

Quality control and assurance in functional near infrared spectroscopy (fNIRS) experimentation

F Orihuela-Espina[1], D R Leff[1], D R C James[1], A W Darzi[1] and G Z Yang[2]

[1] Division of Surgery, Oncology, Reproductive Biology and Anaesthetics (SORA), Imperial College, London, UK
[2] Institute of Biomedical Engineering, Imperial College, London, UK

E-mail: f.orihuela-espina@imperial.ac.uk

Received 5 March 2010, in final form 18 May 2010
Published 9 June 2010
Online at stacks.iop.org/PMB/55/3701

Abstract

Functional near infrared spectroscopy (fNIRS) is a rapidly developing neuroimaging modality for exploring cortical brain behaviour. Despite recent advances, the quality of fNIRS experimentation may be compromised in several ways: firstly, by altering the optical properties of the tissues encountered in the path of light; secondly, through adulteration of the recovered biological signals (noise) and finally, by modulating neural activity. Currently, there is no systematic way to guide the researcher regarding these factors when planning fNIRS studies. Conclusions extracted from fNIRS data will only be robust if appropriate methodology and analysis in accordance with the research question under investigation are employed. In order to address these issues and facilitate the quality control process, a taxonomy of factors influencing fNIRS data have been established. For each factor, a detailed description is provided and previous solutions are reviewed. Finally, a series of evidence-based recommendations are made with the aim of improving consistency and quality of fNIRS research.

(Some figures in this article are in colour only in the electronic version)

1. Introduction

In functional near infrared spectroscopy (fNIRS), the quality of the experiment and of the recovered haemodynamic signals may be compromised in several ways, including modulating the subject's cognitive response, distorting the recorded signals and/or affecting the optical properties of tissues thereby altering path length. There have been many review articles detailing fNIRS principles, technological advances, system design and/or applications (Villringer and Chance 1997, Strangman *et al* 2002, Rolfe 2000, Hoshi 2007, Gibson and

Dehghani 2009, Lloyd-Fox *et al* 2009). However, there have been limited efforts at producing a unified evidence-based framework to ensure the quality of fNIRS experimentation and help guide the novice researcher.

The motivation of this paper is to summarize the factors that may influence the quality of fNIRS experimentation. In addition, evidence-based procedures designed to enhance the quality of fNIRS experimentation are evaluated. This systematic framework for best practice is designed to assist new researchers to appropriately plan, design and evaluate the results of fNIRS experiments. The rapid developments in multimodal imaging (Hoshi 2007) means that this framework is also likely to benefit researchers experienced at other neuroimaging techniques such as electroencephalography (EEG) or functional magnetic resonance imaging (fMRI). The framework focuses on optical topography (OT) as this is currently the most relevant modality for functional neuroimaging studies, although many of the principles covered also apply to optical tomography. Ethical aspects and moral implications are considered beyond the scope of this paper even though they have implications for scientific quality.

2. A taxonomy of experimental factors influencing fNIRS experimentation

A taxonomy of the methodological factors influencing experimental quality in fNIRS is proposed in table 1. In the highest taxonomic rank, the following taxa separate the origin of the factors.

- Environmental: intrinsic to the laboratory.
- Instrumentation: regarding the interplay of the illumination and detection configuration.
- Mechanical: related to the optode manipulation, positioning and coupling.
- Population: as regards cohort demographics and behaviours.
- Physiological: concerning the physical and chemical variables related to human physiology.
- Study design and data analysis: involving generic and fNIRS-specific decisions regarding protocol and analysis.

The manner in which these factors influence experiment quality is depicted in figure 1. For each of these factors (1) we state the evidence for the problem, (2) review solutions and (3) whenever possible suggest procedures to alleviate the problem.

3. Environmental factors

3.1. Ambient light

Optodes refer to the set of transducer, immobilization polymer and instrumentation including the optical fibre and light source that makes the optical sensor. Poor shielding and/or coupling between optode and skin permit ambient light to reach the detectors increasing the optical power or irradiance at the sensor. Optode shielding schemes limit the ability of ambient light to reach the photodetectors (Lloyd-Fox *et al* 2009). Solutions incorporated into devices to reduce contamination by ambient light include the use of long pass filters (Cope and Delpy 1988), lock-in amplifiers (Coyle *et al* 2004), differential detection (Lee 2004) and embedding sensors in foam (Bozkurt *et al* 2005). Sensitivity to ambient light can be reduced by conducting experiments in a dimmed room (e.g. Hoshi *et al* (2005), Holper *et al* (2009) and Schroeter *et al* (2003)) and further attenuated by using a light tight bandage (Wyatt *et al* 1990) or covering the sensors with a dark felt or cloth (Hoshi *et al* 2005, Meek *et al* 1995, Obrig *et al* 2002).

Table 1. Taxonomy of experimental factors influencing fNIRS experimentation.

Class	Family	Genera	Evidence-based best practice
Environmental	Ambient light	Room dimming, optode cover	• Dim laboratory lights • Shield and cover optodes
	Noise level	See attention	
	Laboratory conditions	Temperature, humidity and ventilation	• Carry experiments at room temperature • Avoid extreme conditions
Instrumentation	Illumination system	Laser heating time, cross-talk/wavelength selection, system drift (optode calibration)	• Warm-up lasers at least 30 min prior to data collection • Utilize one wavelength at 830 nm and another between 660 and 770 nm.
	Propagating fibres	Width, length, material and type of the optical fibres, stray-light rejection	• Glass fibres are more flexible, weigh less and provide improved measurements
	Laser safety	Laser power, tissue heating, injury to the skin, injury to the eye	• Laser power must be kept within IEC standard limits • Always protect the eyes of the volunteers
	Detection system	Saturation, electromagnetic noise, emergent light dynamic range	• Data suffering from saturation artefacts must be identified and rejected from further analysis
Mechanical	Interoptode distance	Depth sensitivity, source–detector arrangement	• Typical interoptode distance is 30 mm for adults and 20 mm for infants
	Geometric optode configuration	Optode arrangement, high density arrays, overlapping versus non-overlapping geometries	• High-density multidistance and overlapping geometries can yield a better spatial resolution at the cost of higher reconstruction complexity
	Optode-scalp coupling	Headgear and optode mounting devices, pressure, skin-optode coupling, optode movement	• Ensure adequate stable contact between the optodes and the scalp throughout the acquisition session • Data contaminated by optode movement artefact must be identified
	Optode positioning, location and registration	Registration to standard systems, co-registration to fMRI systems, relocation, distance to targeted scalp location, probe size	• Registration to cortical surface is essential and efforts taken must be reported

Table 1. (Continued.)

Class	Family	Genera	Evidence-based best practice
			• Location of optodes must be made against a standard positioning system
Population	Demographics	Age, gender/sex, ethnicity/race, handedness, past medical history and current medical conditions	• Inclusion and exclusion criteria must be explicitly reported • When appropriate, groups must be matched to minimize the effects of demographic confounders.
	Measurement day particulars	Stimulants intake (caffeine, nicotine, alcohol, other drugs) and attention (noise level, cooperativeness and anticipatory response)	• Intake of stimulants by the cohort must be controlled for at least 24 h. prior to data acquisition
Physiological	Neurovascular coupling	Spatiotemporal linear and nonlinearities and habituation.	• Interpretation of results must be made within understanding of the neurovascular coupling conditions
	Systemic	Heart rate/cardiac pulse, breathing and respiratory rate, arterial pulsation, blood pressure, cerebral circulation and gas exchange and scalp blood flux.	• Physiological interference must be eliminated, reduced or incorporated as confounder during analysis
	Extra-cranial	Scalp blood flux, scalp and skull thickness, hair	
	Intra-cranial	Dura mater, arachnoid, CSF and pia mater	
Study design and data analysis	Protocol design	• Generic: randomization, assumption checking, nonlinear relations, indirect relations, control group/task, population size, • fNIRS specific: paradigm (block versus event-related), number of trials, task length and intensity, rest periods/alternative task, and timings, temporal window for analysis and haemodynamic signal for analysis	• Pilot studies may help to adjust optimum experimentation parameters
	Image reconstruction	Photon transport modelling, MBLL, differential pathlength factor, diffusion theory, temporal versus spatial reconstruction	• Interpretation of results must be confined to the limits imposed by the assumptions made during the image reconstruction.
	Image processing and analysis	Hypothesis-driven versus data-driven analysis framework, data integrity checks, software	• Data integrity checks must follow signal preprocessing

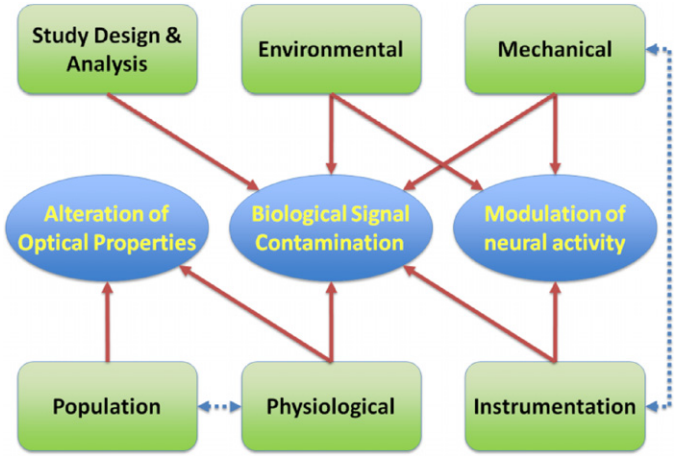

Figure 1. Pathways for how each factor class may compromise experiment quality. Continuous lines link factors to consequences. Dashed lines represent strong interactions between factors themselves.

3.2. Room conditions

Electronic instrumentation works optimally at certain temperatures, levels of humidity and ventilation. Minimizing temperature fluctuations during the experiment reduces system drift and ensures stability of the measuring system (Schmidt *et al* 2000, Haensse *et al* 2005). Manufacturers of OT systems, such as HITACHI, recommend installation and use at controlled temperatures and under humidity conditions so that equipment operation is stable. In addition, extreme room conditions may influence subject's comfort and performance. Some investigators report their laboratory temperature (22–24°) and humidity conditions (40–50%) and methods of ventilation (Tanida *et al* 2007, Kudo *et al* 2008). In general, experiments should be conducted at room temperature.

4. Instrumentation factors

4.1. Illumination system

A range of commercial and in-house systems for fNIRS application have been described (Franceschini *et al* 2006, Yamashita *et al* 1998, Everdell *et al* 2005, Bozkurt *et al* 2005, Haensse *et al* 2005, Cope and Delpy 1988, Schmidt *et al* 2000, Siegel *et al* 1999). Each system possesses a unique illumination and detection configuration. A schematic diagram of a commercial OT-fNIRS system is illustrated in figure 2.

4.1.1. Cross-talk. To recover more than one chromophore (e.g. oxy-Hb and deoxy-Hb), fNIRS capitalizes on the distinct absorption curves of the chromophores to be recovered. The incorrect separation of chromophore changes is known as cross-talk (Uludag *et al* 2002, Strangman *et al* 2003). Cross-talk is mainly affected by wavelength selection, but also by errors in the extinction coefficient used, and the stage at which instrumentation noise and motion artefacts are eliminated (Uludag *et al* 2004, Sato *et al* 2004, Yamashita *et al* 2001, Huppert *et al* 2009). To minimize the degree of cross-talk, the growing consensus is to utilize one wavelength at 830 nm and another one between 660 and 770 nm (Gibson and Dehghani 2009).

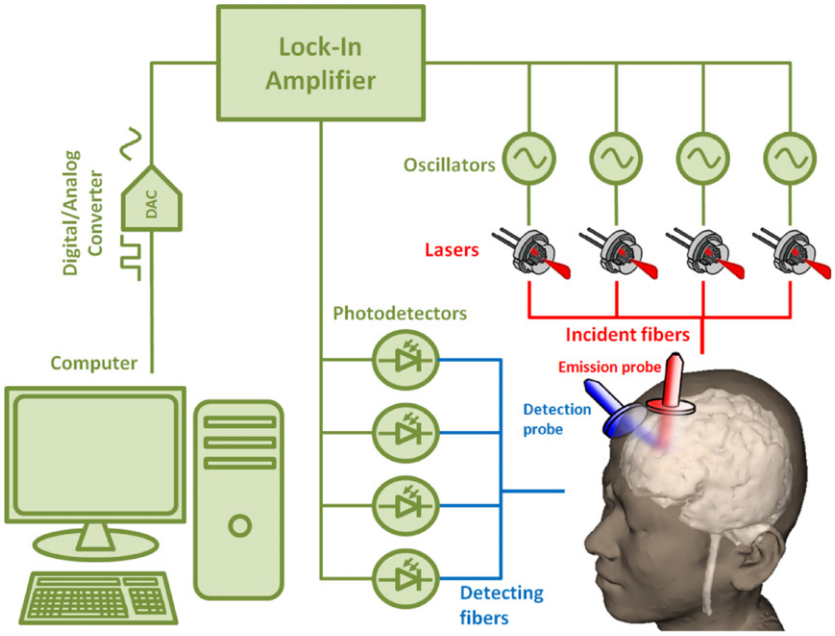

Figure 2. Schematic representation of a functional near infrared measurement system.

4.1.2. System drift and optode calibration. System drift is due to low frequency noise introduced by an electronic instrument which results in poor signal-to-noise ratio (SNR) for repeated measurements. Optode calibration methods regulate the strength of the light sources, automatically adjust the gain of the detectors, determine initial optical properties and boundary conditions and remove errors from model mismatch. A number of calibration algorithms have been proposed for all the three NIRS modalities: time-resolved (e.g. Hebden *et al* (2003)), frequency domain (e.g. Li and Jiang (2004)) and continuous-wave (e.g. Stott *et al* (2003)). For continuous wave systems, a simple normalization may suffice as an alternative to calibration procedures (Huppert *et al* 2009). Linear detrending is a simple solution to eliminate system drift, consisting of fitting a first-degree polynomial to baseline samples and subtracting it from the signal. Optode calibration methods ensure optimal gain of receptors, and in addition they can partially compensate for gradual movement of the optodes, and ambient light contamination.

4.1.3. Laser heating time and life. Light sources in NIRS applications employ either laser or light emitting diodes (LED) sources. Cold lasers do not perform optimally. Thus, operating with cold lasers results in a reduced SNR and interference with optode calibration. Reported laser warm-up times range from 30 min up to 10 h (Haensse *et al* 2005, Schmidt *et al* 2000). Thermoelectric coolers permit thermal control of the laser for optimum performance (Williams 2001). In addition, as the lifetime of the laser expands their luminosity fades and their performance decreases. It is advisable to switch on the lasers at least 30 min prior to data acquisition.

4.2. Propagating fibres

The type, material, width and length of the fibres propagating the illumination to the tissue may distort light profile and deviate from nominal measurement wavelengths. The propagation

velocity of light travelling through the fibre is wavelength dependent, resulting in wavelength-specific delays. The more the illuminating profile differs from the nominal, the greater is the need for stray-light rejection (Siegel *et al* 1999). Longer fibres can increase subject mobility, and the attenuation suffered by light in short distances within a laboratory may be neglected. Although glass fibres are expensive, they are more flexible, weigh less and provide improved optical measurements than other materials (Lloyd-Fox *et al* 2009).

4.3. Laser safety

Safety in fNIRS systems imposes restrictions on the way the NIRS imaging devices are used. The International Electrotechnical Commission's (IEC) report states that light in the wavelength range 400–1400 nm has the potential to cause photochemical and febrile damage to the retina, and cataract, as well as to inflict retinal and skin burns (IEC 2007).

4.3.1. Injury to the skin. NIR light is non-ionizing but it is transferred to thermal energy following absorption (Ito *et al* 2000). The combined effect of radiated and conducted heating characterizes the increase in tissue heating, which quickly decreases with depth and deviation from the irradiation point. Maximum permissible exposure (MPE) of the skin against laser radiation is 3.3 mW mm^{-2} for two wavelengths, so optical fibre output is permitted up to 31.4 mW. However, the exact limits of maximum radiation depend on many factors including emission wavelength, light coherence, exposure time, area being illuminated, light beam characteristics and the absorption and scattering properties of the tissue, as well as the subject's skin tolerance, e.g. neonates and albinos are special groups at risk. Exceeding safe power limits will result in tissue heating and in extreme cases in thermal necrosis (Siegel *et al* 1999). Commercial devices often work well below the MPE threshold. For instance, the ETG-4000 (Hitachi Medical Corporation) optical fibre output is set to 3 mW that is 1/10 of the MPE. For high precision analysis, thermally induced alterations of the optical properties of the tissue can be modelled with energy transport models.

4.3.2. Injury to the eye. Eye lens directs the light beam into the fovea, which receive a potentially harmful stronger irradiance. Most fNIRS devices operate at power levels consistent with Class 1M lasers (safe as the blink reflex prevents ocular exposure for more than 0.25 s) according to IEC safety standard (IEC 2007). However, caution should be taken to avoid inadvertent eye exposure since the threshold to avoid ophthalmic injury is substantially lower than that for the skin. It is desirable that the lasers are not switched on until the optodes are in contact with the subject's scalp, but volunteer discomfort and laser warm-up times may prove this unfeasible. An alternative strategy is to ask subjects to close their eyes or to use eye protection during optode placement.

4.4. Detection system

Scintillation light detectors commonly employed in fNIRS are either photomultiplier tubes (PMT), conventional silicon photodiodes (SPD) or avalanche photodiodes (APD). Regardless of the scintillator and the mode of operation of the detector (pulse or current), the output from the sensor may become saturated due to the high optical power or irradiance—commonly by exposure to ambient light, the applied voltage bias, saturation of the circuit parts, ambient electrical/magnetic noise or radio waves emitted by devices such as cell phones. For time-resolved apparatus, power supply stability, optical reflectance, data acquisition efficiency, temporal accuracy and laser pulse stability may also adversely influence light detection

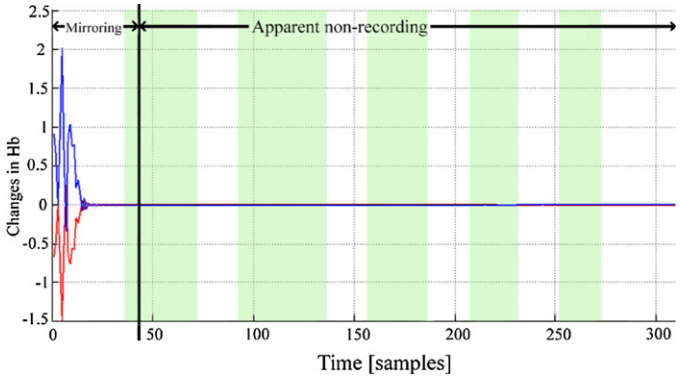

Figure 3. Detector saturation artefacts. Example of experimental data showing changes in hemoglobin species HHb (blue line) and HbO_2 (red line) under saturation artefacts. The shaded patches correspond to self-pace surgical knot-tying task blocks. The first stage is only affected by the saturation at one of the acquisition wavelengths, and the mirroring effect is clearly observable. From there onwards, the detector also gets saturated at the second wavelength and a non-recording effect appears.

(Schmidt *et al* 2000). In a two-wavelength system reconstructed with the modified Beer–Lambert law, if only one wavelength is saturated the concentration changes in oxygenated and deoxygenated haemoglobin are related by a negative constant, an effect referred to as 'mirroring'. If both wavelengths are saturated, changes in concentrations become zero, an effect that we call 'apparent non-recording'. Figure 3 illustrates common artefacts induced as a result of detector saturation.

Strategies to detect saturation artefacts include thresholding raw light data stream before conversion to chromophore concentration (Huppert *et al* 2009) or spectral analysis (Blasi *et al* 2007). Capitalizing on the numerical solution of the modified Beer–Lambert law (MBLL) differential system of equations, our practice is to apply a multiscale cross-correlation algorithm to detect saturation. In systems where a large variation of source–detector distances is permitted, the dynamic range of the intensity of the emergent light will be very large. In this instance, variable optical attenuators are necessary to avoid saturation or even damage to the detectors (Schmidt *et al* 2000, Haensse *et al* 2005). Huppert *et al* (2009) recommend eliminating instrumental noise before conversion of light to haemodynamic data so the error does not propagate. Channels suffering from saturation artefacts should be identified, and these data rejected from further analysis.

5. Mechanical factors

5.1. Interoptode distance

The diffuse nature of photon migration within the tissue limits the depth of light penetration (Boas *et al* 2004, Franceschini and Boas 2004). Depth sensitivity depends on the illumination strength and optical properties of the tissues in the light path including the concentration of the chromophores. Infrared light can only penetrate up to 8 cm in neonates (Wyatt *et al* 1990) and 7 cm for adults (Villringer and Chance 1997). For planar imaging, relying on backscattered photons, the depth achieved is a function of the interoptode distance and the fibre orientation with respect to the tissue entrance plane (Thilwind *et al* 2009). If the interoptode distance

is too small, the acquired signal will originate from extra-cerebral structures. Conversely, if the source and detector are widely separated, i.e. distances exceeding 40–50 mm, then relatively little light reaches the detectors and signal quality is degraded. If beam entrance is perpendicular to the tissue, a typical source–detector separation when measuring the brain haemodynamics in adults is 30 mm (e.g. Watanabe *et al* (1996), Okada and Delpy (2003b), Sato *et al* (2006b) and Obata *et al* (2003)), which is also optimum for measuring the fast optical signal (Gratton *et al* 2006, Franceschini and Boas 2004). At the 30 mm distance the contribution of the grey matter to the light absorption has been estimated in the order of 20–30% (Toronov *et al* 2000). Smaller source–detector separations are also popular, e.g. 25 mm (Zee van der *et al* 1992) especially in infants (e.g. 20 mm).

5.2. Geometric configuration of optodes

The position and configuration of light sources and detectors on the scalp determine the cortical region(s) under surveillance and limit the accuracy and resolution of the reconstructed image. At a given source–detector separation, paths closer to the surface are shorter and denser than deeper paths. Overlapping geometries, where several channels interrogate the same region, and high density arrays providing multidistance measurements provide better image quality and spatial resolution than non-overlapping single distance geometries (Boas *et al* 2004, Dehghani *et al* 2009b, Yamamoto *et al* 2002, Saager and Berger 2008). However, with single distance non-overlapping geometry the topographic images may be recovered by simple interpolation. Explicitly reporting optode arrangement is a common practice among investigators.

5.3. Optode–scalp coupling

Optode–skin/scalp coupling refers to the tightness and stability of the optode's position with respect to the scalp. Variations in this coupling result in changes in the detected light intensity. Gradual optode movement leads to slow changes that may mistakenly be interpreted as system drift. Abrupt optode movements, also referred to as 'body movement' artefact, manifest themselves as large sudden changes in chromophore concentration, distinct from genuine changes due to cortical activity and more irregular than system noise (Sato *et al* 2006c).

5.3.1. Headgear. The headgear in which the optodes are mounted should ensure good optode–skin coupling and subject comfort. A variety of devices to house the NIR optodes have been described including thermoplastic shell or splint moulds (Takahashi *et al* 2000), steel tubes affixed to a metal frame (Toronov *et al* 2000) and aluminium shells (Blasi *et al* 2007). Mechanical stabilization of the optodes has been attempted by anchoring the optical fibres to a backpack or harness (Huppert *et al* 2009), inserting foam (Bozkurt *et al* 2005), employing integrated source–detector bundles (Hebden *et al* 2003), prism-ended optodes (Lloyd-Fox *et al* 2009), head rests (Meek *et al* 1995) and/or Velcro tape (Franceschini *et al* 2006). In general, whilst higher pressure between optodes and skin provides more stable coupling, excessive pressures induce volunteer discomfort or at worse skin necrosis (Edwards 1995). The excessive pressure can be eased by means of spring-loaded optodes. Index matching gels are used to enhance the coupling with the fibres in other optical applications, but to our knowledge, these are not in widespread use in functional NIRS studies. Despite enhancing stability, the headgear alone is unlikely to completely eliminate all optode movement artefacts.

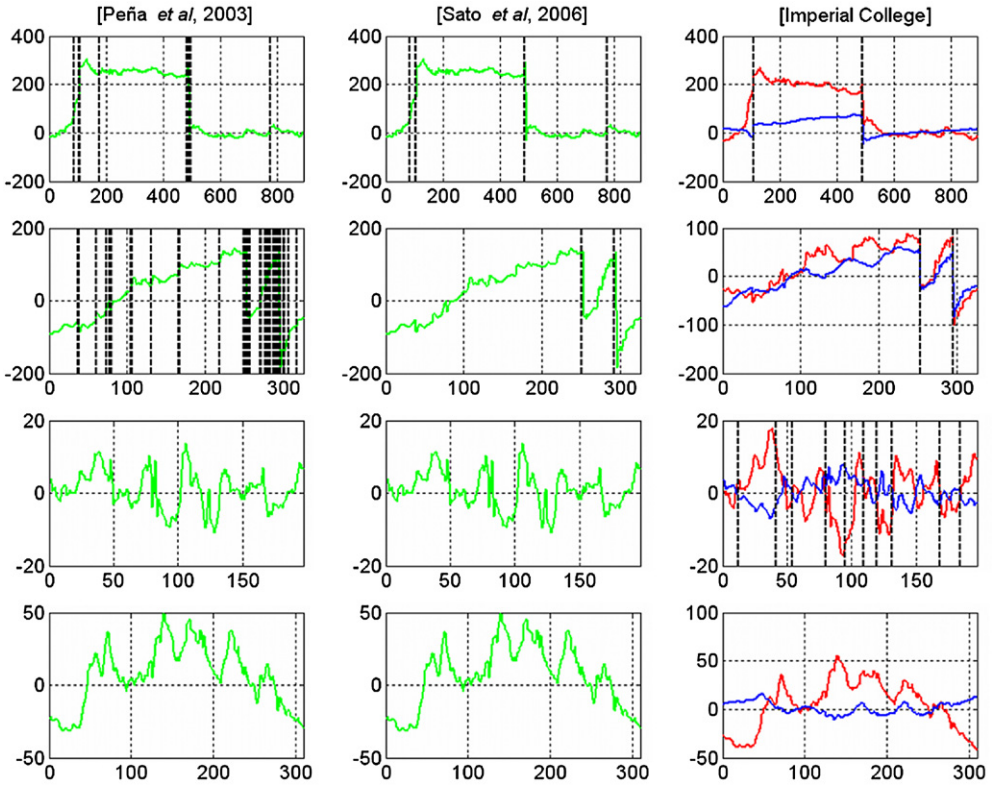

Figure 4. Comparison of different approaches for optode movement detection at different scales. HHb: blue line; HbO_2: red line; total Hb: green line. Units of concentration changes are in μM $\times$ cm. The abscise axis represents time courses in seconds. The different rows represent response of different amplitude. The first column corresponds to detection by two consecutive large changes (Peña *et al* 2003). The second column uses Haar wavelets to look for steps in the signals (Sato *et al* 2006c). The third column defines a flexible region using a double exponential smoothing (Orihuela-Espina *et al* 2008).

5.3.2. Optode movement. Optode calibration methods may alleviate the signal contamination induced by gradual optode movement but will still fail to compensate for the abrupt changes in NIR signals brought about by a loss of optode–scalp coupling. To pinpoint abrupt optode movement, some investigators rely on visual inspection (e.g. Diamond *et al* (2009) and Nakano *et al* (2009)), which is subjective, time consuming and prone to errors. Generic algorithmic solutions for edge detection such as Sobel's mask or Laplacian of a Gaussian can provide good sensitivity but low specificity. Algorithmic solutions specific to fNIRS include discarding two consecutive differences in the changes in total haemoglobin larger than a hard threshold (Peña *et al* 2003), the use of Haar wavelets (Sato *et al* 2006c), PCA truncation (Wilcox *et al* 2005), local and global assessment of the variance (Holper *et al* 2009, White *et al* 2009), ICA over co-located channels (Robertson *et al* 2010), Kalman filtering (Izzetoglu *et al* 2010) and exploiting negative correlations among Hb species (Cui *et al* 2010). Our current practice is to perform visual exploration data integrity checks followed by employing an in-house algorithm based on a soft threshold upon a double exponential smoothing signal model to detect data contaminated with artefact, in order to discard it. Examples of optode movement detection algorithms are illustrated in figure 4. Signal compensation may be necessary to avoid

discarding data from studies with small cohorts. Finally, subtle changes in haemodynamics caused by head motion can be removed using accelerometers and a Wiener adaptive filter (Izzetoglu *et al* 2005).

5.4. Optode positioning, location and registration

Accurate positioning of NIR optodes onto the scalp surface ensures that sampled data originates from the cortical region(s) of interest. Conversely, errors in optode positioning or misalignment of optodes can potentially lead to invalid conclusions regarding cortical function. Typically, optodes are guided into position using the International 10/20 system for optode placement or an equally valid alternative reference in which more cranial positions are defined such as the UI 10/10 or 10/5 systems (Jurcak *et al* 2007). Registration permits mapping the location of optode and channels on the scalp surface to underlying anatomical location on the cortical surface. This is extremely valuable for fNIRS which does not incorporate anatomical information per se. Moreover, registration realizes reproducible measurements across subjects, studies and laboratories, and facilitates comparison of data acquired across different neuroimaging modalities.

Whilst the positioning systems are standardized, there is a considerable heterogeneity regarding the range of implementation and solutions for registration. The current gold standard is co-registration with magnetic resonance anatomical data, which involves placing fiducial markers such as fatty pine nuts (Okamoto *et al* 2004), vitamin capsules (Hatakenaka *et al* 2007) or Beekley Spots® (Gratton *et al* 2006) over optode locations such that the cortical region underlying each optode can be determined from individual subject high resolution MRI images. However co-registration may prove costly and difficult especially in infants. An alternative approach is to use a digitizer to determine 3D locations (Singh *et al* 2005) which are then projected onto a brain atlas. Virtual registration negates the need for 3D digitizers (Tsuzuki *et al* 2007) although this technique is not in routine use at present. To quantify the discrepancy between the intended cranial marker and the location where the measurement was actually recorded, our current approach is, following 3D position digitization, to deform a hemi-spheric mesh representing a standard positioning system and compute the distance from either the real optode location or real channel location to the intended target location, as illustrated in figure 5. A threshold chosen upon the spatial resolution and the interoptode distance is then used to justify data rejection.

Capitalizing on the basis that probabilistic cortical anatomy underlying each standard location has been established unequivocally (Okamoto *et al* 2004), some authors do not report any registration effort (Herrmann *et al* 2008). Others report the registration for a subset of the cohort assuming internal positioning consistency (Leff *et al* 2008a) or occasionally the results for the entire cohort (Gratton *et al* 2006). Neglecting to perform and report registration should be discouraged. It is preferable to report the registration technique, and the degree of misalignment between intended and actual channel locations.

6. Population factors

6.1. Demographics

Cohort selection criteria, i.e. inclusion and exclusion, are defined for both safety and scientific reasons (Ottevanger *et al* 2003). In group studies, investigators should aim to match the groups to reduce the effect of demographic confounders. Restriction of eligibility makes extrapolation

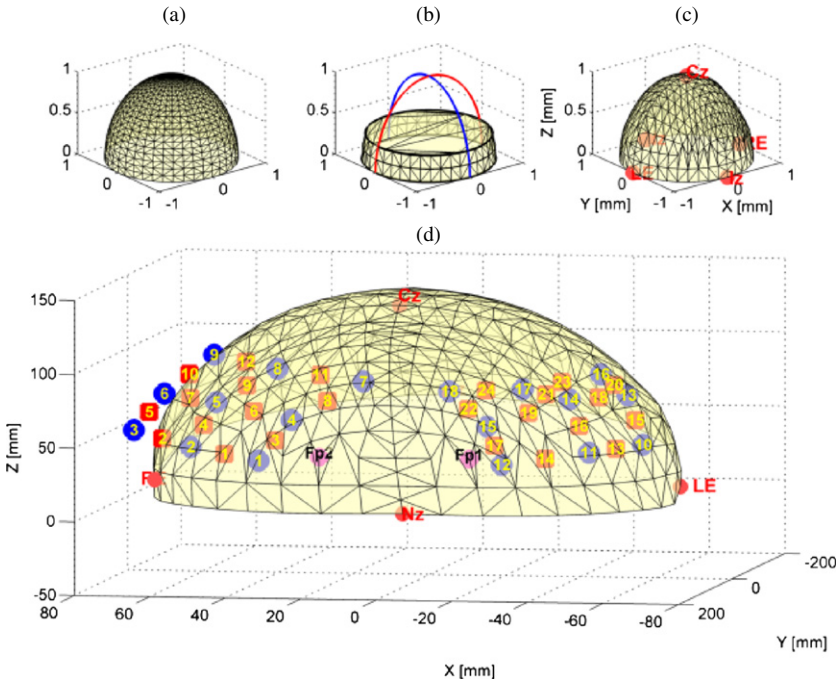

Figure 5. Optode registration. A hemi-sphere representing a standard location system e.g. 10/20, UI 10/10 or 10/5 is deformed to fit five control points (red dots and labels). Distances can then be computed in real world units. Under the assumption of a one-to-one match between the standard locations and associated cortical regions, the imaged cortical area can be established. (a) A hemi-sphere mesh (semi transparent yellow mesh) yet to be deformed; (b) sagittal (Nz-Iz)—blue—and coronal (T9-T10)—red—axes and the 0%, 5% and 10% axial reference curves; (c) mesh deformed according to the 3D digitized location of five control points (Nz, Iz, T9, T10 and Cz); and (d) an example on real data showing the 3D locations of optodes (blue circles), estimated channels positions (red squares) and some target standard locations (magenta dots).

hazardous and increases the complexity of the experiment. Exclusion and inclusion criteria should be described in detail.

6.1.1. Age. Senescence-induced cortical atrophy results in changes in the tissue optical properties, which in turn affect the depth of penetration (Svasaand and Elligsen 1983), optical pathlength (Kameyama *et al* 2004), partial volume and cross-talk (Schroeter *et al* 2003). In addition, cortical responses in older subjects have been observed to be less pronounced versus their younger counterparts (Herrmann *et al* 2006, Mehagnoul-Schipper *et al* 2002). The age range or mean age of the recruited cohort and/or groups of interest must be reported. If significant age differences exist between groups of interest, then the effect of age should be considered as a confounding or independent factor (Herrmann *et al* 2006).

6.1.2. Gender. Gender reorganizes brain activity (Kameyama *et al* 2004, Herrmann *et al* 2006). Investigators commonly report the sex distribution of the study participants (e.g. Leff *et al* (2008a), Sato *et al* (2006b) and Plichta *et al* (2007a)), but few reports describe matching to eliminate sex-related confounds.

6.1.3. Ethnicity. Light absorbed by the scalp is a function of skin colour. Melanin concentrations and composition in the skin and hair greatly vary across race (Alaluf *et al* 2002). Moreover, changes in blood pigments are more difficult to observe in the presence of high concentrations of melanin. Notwithstanding, reporting ethnicity of the cohorts is uncommon.

6.1.4. Handedness. The dominance of the left and right cerebral cortex for tasks such as spatial cognition, speech and language is related to handedness. Handedness is most commonly evaluated using a validated scale such as the Edinburgh Inventory handedness (Oldfield 1970).

6.1.5. Past medical history and current medical conditions. Many studies report that their volunteers are healthy (e.g. Higashi *et al* (2004), Toronov *et al* (2000) and Mehagnoul-Schipper *et al* (2002)) and/or have no psychological or psychiatric history (e.g. Kameyama *et al* (2004) and Sato *et al* (2006b)). Many other medical conditions can influence optical signals, for instance by directly altering the CBF or the systemic response, causing cognitive impairment and/or inducing neurodegeneration, e.g. cardiac diseases, diabetes mellitus, HIV/AIDS, migraine and gestational hypertension disorders. Vasodilator medication can help to normalize CBF in hypertension (Pieniążek *et al* 2001).

6.2. Measurement day particulars

6.2.1. Stimulant intake. Stimulants alter the way in which the brain responds to stimuli. Caffeine increases metabolism while at the same time induces cerebral vasoconstriction, decreases the CBF and modulates brain activity (Higashi *et al* 2004, Dager and Friedman 2000). Nicotine increases CBF and, when combined with caffeine, may result in increases in heart rate and blood pressure, i.e. alterating the systemics (Dager and Friedman 2000). Cerebral autoregulation may maintain CBF in the face of moderate and even acute alcohol intake but alcohol may alter certain higher order brain functions (Obata *et al* 2003). Other drugs have the potential to confound haemodynamic responses (Ladewig *et al* 2002, Hasan *et al* 2009). Effects of chronic or sustained abuse of certain substances may transcend the day of intake. Experimenters should control for the intake of stimulants by the study cohort. Our practice is to request that participants refrain from drinking alcohol and ingesting caffeine for 24 h prior to data acquisition.

6.2.2. Attention. Attention regulates the activity of brain circuits (Herrmann *et al* 2008). Noise in the laboratory may distract the subject, divert their attention from the task at hand and at worse confound imaging data (Abdelnour and Huppert 2009). Physical and psychological fatigue can further modulate the brain response (Suda *et al* 2009, González-Alonso *et al* 2004). Insufficient attention to the task is common when working with infants who may cry, refuse to wear the probes or simply fail to attend to visual stimuli (Taga *et al* 2003, Watanabe *et al* 2008). Maximizing cooperativeness during data acquisition is essential. Solutions include ensuring that background noise is kept to a minimum by conducting the experiment in a quiet room. Using alternative tasks during rest periods may help to maintain attention and focus. Data acquired when attention to the stimulus is deemed insufficient or unsatisfactory should be discarded. Anticipatory activation may be generated before repeated predictable events (Nakano *et al* 2008) or as a result of anxiety (Morinaga *et al* 2007).

7. Physiological factors

7.1. Neurovascular coupling

Neurovascular coupling describes the way in which neuronal activity translates into changes in CBF, cerebral blood volume (CBV) and regional cerebral metabolic rate of oxygen ($CMRO_2$). There exist a number of models for approximating the CBF, CBV and $CMRO_2$ from fNIRS measurements (Wyatt *et al* 1990, Boas *et al* 2003). The relationship between neuronal activation and the vascular response is neither temporally nor spatially constant (Obrig *et al* 2002, Devor *et al* 2005, Sheth *et al* 2004). Habituation, a decrease in the response either neural or vascular (Obrig *et al* 2002, Krekelberg *et al* 2006), may occur within and across trials and can be sustained from minutes to days (Nakano *et al* 2009). Interpretation of measured brain haemodynamics must be made with good comprehension of neurovascular coupling, and the conclusions extracted must be bounded by the assumptions made over this physiological process, such as linearity.

7.2. Systemic effect

Systemic signals such as arterial pulsation, blood pressure, vasomotion, basal cerebral circulation, respiratory rate, gas exchange and scalp blood flow are known to influence changes in cortical haemodynamics despite cerebral autoregulation (Elwell *et al* 1994, 1999, Diamond *et al* 2006, Obrig *et al* 2000, Franceschini *et al* 2006). In contrast to the localized response due to the neurovascular coupling, the systemic response influences haemodynamics globally. As illustrated in figure 6, cortical haemodynamic signals may be contaminated at various frequencies with systemic artefacts. Classical filtering will fail to remove systemic oscillations with overlapping frequencies. Solutions to quantify, account for and/or remove systemic artefacts can be classified as follows:

- blind source separation when no concomitant systemic signals are available or acquired (Zhang *et al* 2005b , Katura *et al* 2008, Virtainen *et al* 2009);
- model-based incorporating prior knowledge (Abdelnour and Huppert 2009, Diamond *et al* 2006);
- adaptive filtering using systemic physiological data acquired simultaneously with fNIRS, either by means of multidistance acquisition (Saager and Berger 2008) or using auxiliar technologies (Kohno 2007).

The exact extent to which systemic signals contaminate fNIRS data still remains under investigation (Katura *et al* 2006). Whenever possible, it is preferable to eliminate systemic interference to reduce false positives (Tachtsidis *et al* 2009).

7.3. Extra-cranial

Extra-cranial contributions to the signal affecting the optical pathlength include aspects of variable anatomy (tissue and skull thickness) and the presence and colour of hair (Okada and Delpy 2003b, Strangman *et al* 2002)—scalp blood flow is considered part of the systemic effect. Extra-cranial contributions vary across subjects and head locations. In frequency-domain NIRS, the concentration changes derived from phase change values are more sensitive to deeper layers, hence naturally minimizing extra-cranial contamination (Obrig *et al* 2002). Dense hair-bearing regions of the scalp decrease the optode grip and reduce optode scalp coupling. Dark hair pigmentation and the presence of hair follicles may reduce the intensity of the signal, by as much as 20–50% (Koizumi *et al* 1999). The simplest solution is to carefully

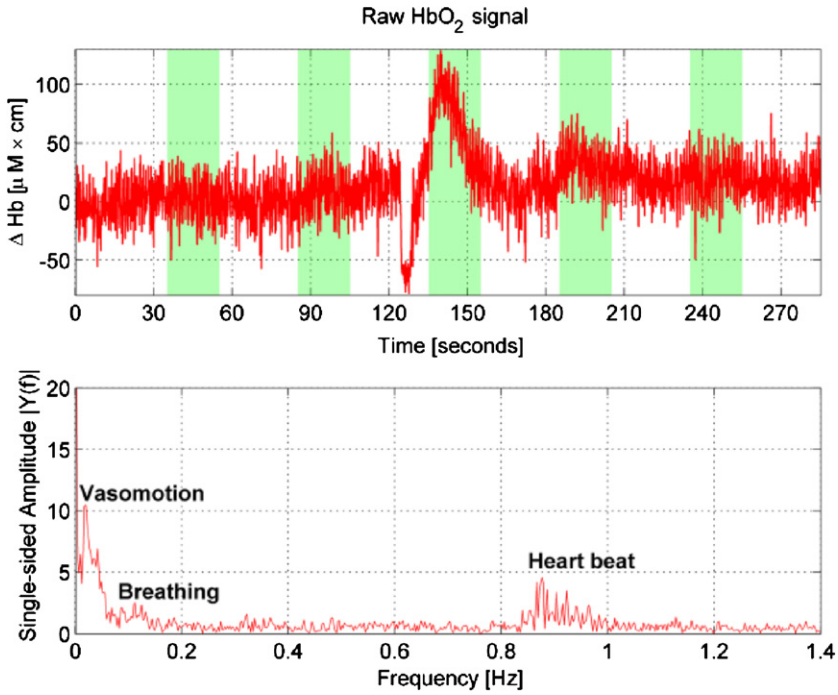

Figure 6. The effect of systemic variables on the haemodynamic signal. The upper plot represents the raw HbO_2 signal after reconstruction using the modified Lambert law, but without any further processing. The lower plot illustrates the Fourier transform of this signal to the frequency domain. Peaks for vasomotion, breathing and heart rate can be easily appreciated.

comb hair away from below the optodes or in extreme cases reject data exhibiting low SNR secondary to hair obstruction (e.g. Watanabe *et al* (2008) and Nakano *et al* (2009)).

7.4. Intra-cranial

Intra-cranially, light crosses the dura mater, the arachnoid layer, the cerebrospinal fluid (CSF) and finally the pia mater before reaching the cortex. It is adequate to consider the meninges as a single homogenous CSF layer (Okada and Delpy 2003b, Hoshi *et al* 2005, Custo *et al* 2006). Photons are strongly affected by this homogenous CSF layer, influencing the optical pathlength and change in the depth of the sensitivity profile (Okada and Delpy 2003a, 2003b).

8. Study design and data analysis factors

8.1. Protocol design

The study design and analysis strategy often go hand in hand and are directly relevant for correct interpretation of results. fNIRS researchers face generic decisions regarding designing task and control paradigms, appropriate randomization, selection of population size and appropriate use of inferential statistics including assumption checking and results interpretation (Ottevanger *et al* 2003, Petersson *et al* 1999a, 1999b). However, fNIRS investigators face additional decisions regarding specific parameters of the experiment: specifically, (i) the data acquisition

paradigm, (ii) the number of trial repetitions, (iii) the length and intensity of the stimulus and subsequent recovery periods, (iv) the definition of the rest periods or alternative tasks, (v) the temporal window for baseline/task data analysis and (vi) whether to analyse only one haemoglobin species, both, or a derivate measure such as total haemoglobin (HbT). In our experience, it is useful to conduct pilot studies to adjust protocol design parameters as well as to identify shortcomings likely to arise during data acquisition.

8.1.1. Data acquisition paradigm. In a block design, similar events are grouped or separated into different data acquisition sessions, whereas in an event-related design, events are mixed and acquired in a single session. The block design is more efficient for detecting differences between stimuli because it maximizes the predictor variance although is more affected by physiological noise and anticipation (Lloyd-Fox *et al* 2009, Nakano *et al* 2008, Morinaga *et al* 2007). Event-related designs are superior at coupling brain activity to specific events, therefore allowing more precise inferences. Event-related designs are useful if the task of interest cannot be repeated rapidly and have been shown to exhibit reliability and reproducibility of the signal at a group level (Plichta *et al* 2006, 2007b).

8.1.2. Number of trials. The number of trials is a compromise between the SNR, habituation and subject comfort. Single trial designs may be insufficient to yield reliable responses due to poor SNR but effects of habituation can be expected from as early as the fifth trial (Nakano *et al* 2009, Lloyd-Fox *et al* 2009). In addition, from our own experience, sessions lasting more than 15–20 min (including optode positioning and registration time) can become tiresome for adult volunteers.

8.1.3. Length and intensity of the stimulus and subsequent recovery periods. The observed haemodynamic response is dependent on the duration of both stimulus and the inter-trial intervals (Obrig *et al* 1997, Toronov *et al* 2000). For a long stimulus, the HbO_2 signal may reach a plateau that it is maintained until the cessation of the stimulus (Heekeren *et al* 1997). If the inter-trial interval is small, the pre-stimulation baseline may reflect post-stimulus changes from the previous trial. Longer inter-trial intervals lead to prominent HHb overshooting (Obrig *et al* 1997). The intensity and/or complexity of the stimulus further modulate the strength of the haemodynamic response and may even determine the recruited brain circuitry (Suzuki *et al* 2004).

8.1.4. Definition of the rest periods or alternative tasks. A rest period of complete mental/motor inactivity is desirable to provide a reliable baseline. For visual stimulation, the rest period usually involves switching the monitor to a black screen (Plichta *et al* 2006). However, maintaining mental inactivity may be challenging. For example, one cannot enforce inactivity in infants and so alternative tasks must be designed, such as attracting an infant's attention with animated cartoons during rest periods (Blasi *et al* 2007).

8.1.5. Temporal window for analysis. Temporal window selection for data analysis may be the difference between success and failure of detecting brain activity. Researchers often analyse the time to peak of HbO_2 or the time to nadir of HHb (e.g. Watanabe *et al* (2008)). However, these variables are prone to large inter subject and inter task variation (Obrig *et al* 1997). Temporal window selection or period where activation is looked for can be fixed (same onset and duration across all subjects and trials) or floating (variable onset and/or duration incorporate the time to peak or nadir, respectively) (Sato *et al* 2006b) and can either be aligned

with the onset of the stimulus or delayed (usually 3–5 s). Furthermore, the selected window may or may not extend beyond the duration of the stimulus itself in order to capture the peak response, thus incorporating rest data as stimulus data. Temporal normalization may be appropriate for self-paced tasks before selecting a temporal window for analysis (Leff *et al* 2007). Currently, there is a lack of consensus regarding the most suitable temporal window for analysis.

8.1.6. Haemodynamic signal for analysis. The classical haemodynamic signature of brain activity as detected with fNIRS is an increase in HbO_2 and a concurrent decrease in HHb, together with an increase in HbT. Multivariate analysis is possible but is usually complex. Many authors prefer to address functional questions in terms of only one Hb species, i.e. one variable. The decision of which variable to use is not trivial. HbO_2 has been said to be the most sensitive indicator of regional CBF in NIRS measurements (Hoshi *et al* 2001), but HHb better reflects the match between oxygen supply and demand (Elwell *et al* 1994). Also, physiological noise is more prominent in HbO_2 (Obrig *et al* 2002). Furthermore, due to cross-talks, the recovery of both signals is to some extent affected by their counterpart. Even when both haemoglobin signals are considered, the statistical analysis is actually performed as two independent univariate analyses (e.g. Sato *et al* (2007) and Plichta *et al* (2006)), rather than being multivariate. Optical neuroimaging is also capable of detecting the terminal enzyme of the respiratory chain, known as cytochrome oxidase (Jöbsis *et al* 1977, Rolfe 2000). Although it is arguably the most specific to brain activity, its measurement is more complicated than that of the vascular parameters, mainly because the amplitude of the signal is at least one order of magnitude smaller than that of haemoglobin (Greisen 2006).

8.2. Image reconstruction

With fNIRS, changes in light intensity only (continuous wave), intensity and phase (frequency domain) or time of flight (time resolved) are monitored to reconstruct the cortical haemodynamics. Image reconstruction refers to the problem of recovering meaningful chromophore concentrations from detected light measurements (Arridge *et al* 1997). Image reconstruction is critical and ultimately determines the spatial and temporal accuracy of the haemoglobin concentration recovered. The theory or model adopted to solve this inverse problem varies according to the imaging modality and requires a trade-off between assumptions made, complexity and computational burden (Arridge *et al* 1997, Hebden *et al* 1997, Dehghani *et al* 2009a).

Concerning OT, the MBLL (Delpy *et al* 1988) is almost universally applied to image reconstruction. The MBLL ignores light polarization and assumes elastic scattering, independent effect from the absorbers, monochromatic radiation, a non-changing source detector configuration and a constant homogenous medium geometry. Due to the unknown scattering properties, the MBLL cannot recover absolute Hb concentration values, but rather changes in concentration upon differential formulation. The differential pathlength factor (DPF) in the MBLL accounts for the increase in the optical path length caused by intense scattering of photons in biological tissues (Delpy *et al* 1988, Zee van der *et al* 1992, Duncan *et al* 1995, Sato *et al* 2006a, Kohl *et al* 1998). The DPF is known to vary with wavelength (Essenpreis *et al* 1993), interoptode distance (Zee van der *et al* 1992) and penetration depth—for a fixed interoptode distance (Hemelt and Kang 1999). A common approximation is to represent the DPF by a single value, e.g. 5.93 for adults and 3.85 for infants (Zee van der *et al* 1992), but such a crude approximation has been criticized (Okada and Delpy 2003b). Other

researchers do not apply DPF correction and work with relative changes in Hb concentration (e.g. Nakano *et al* (2008) and Leff *et al* (2008a)).

8.2.1. Temporal versus spatial reconstruction. Reconstruction is usually spatial, not temporal, i.e., the solution to the inverse problem is computed at every time point (Zhang *et al* 2005a). To directly model the temporal dynamics of the chromophores, a haemodynamic response function (HRF) model must be convolved with the stimulus train. While HRF models are widely applied in fMRI, not until recently has an HRF specific to optical imaging been proposed (Zhang *et al* 2005a, Akin and Bunce 2003) and some models now accept temporal basis functions as inputs (Diamond *et al* 2006).

8.3. Image processing and analysis

De facto standard processing of fNIRS signals includes low-pass or band pass filtering to remove instrumentation noise, detrending to eliminate system drift and averaging across trials to increase SNR (Huppert *et al* 2009, Lloyd-Fox *et al* 2009). Data integrity checks, or signal assessment, detect and/or eliminate artefacts not rectifiable using such standard processing framework and ensure that only appropriate clean signals are allowed to be analysed further. Approaches to data integrity include visual assessment, or systematic algorithmic checks. Several software packages for fNIRS image reconstruction and signal processing are already available:

- HomER (Hemodynamic Evoked Response) (Huppert and Boas 2005) (http://www.nmr.mgh.harvard.edu/PMI/resources/homer/home.htm).
- fOSA (function Optical Signal Analysis) (Koh *et al* 2007) (http://www.fil.ion.ucl.ac.uk/spm/).
- TOAST (Time-resolved Optical Absorption and Scattering Tomography) (http://web4.cs.ucl.ac.uk/research/vis/toast/index.html).
- ICNA (Imperial College Neuroimage Analysis) (Orihuela-Espina *et al* 2009).
- NIRS-SPM (NIRS Statistical Parametric Mapping) (Ye *et al* 2009) (http://bisp.kaist.ac.kr/NIRS-SPM.html).

A classical dichotomy considers analysis techniques as either hypothesis driven or data driven. Well-established hypothesis-driven frameworks from other neuroimaging modalities such as the general linear model and its variant statistical parametric mapping are now being adapted for fNIRS application (Plichta *et al* 2007a, Koh *et al* 2007). New data-driven approaches, such as manifold embedding (Leff *et al* 2007) and Markovian modelling (Leff *et al* 2008b), are expanding the range of analysis options. We favour a combination of analysis strategies, developing new data-driven solutions and validating findings using classical inferential statistics.

9. Conclusions

The quality of an fNIRS experiment and the acquired data may be compromised due to errors in methodology adversely affecting the optical signal. In this paper, we have defined a taxonomy of factors that need to be considered to ensure quality in fNIRS experimentation. Each of these factors has been systematically approached in a three-step strategy: (i) factor description, (ii) evidence-based solutions overview and (iii) conclusions or recommendations based on the former two.

Effort toward excellence in fNIRS research has led to significant improvements in quality by following good experimental practices and protocols for data acquisition, ensuring appropriate quality assessment and formulating criteria for reporting outcomes. However, as highlighted in this work, these efforts seem to be poorly coordinated and often inconsistent, with several aspects still necessitating a consensus among fNIRS researchers. Further research should help define standard operating procedures to enhance methodological quality, increase reliability and consistency in result reporting, assist researchers new to fNIRS and improve cohesion amongst different optical imaging laboratories.

References

Abdelnour A F and Huppert T 2009 Real-time imaging of human brain function by near infrared spectroscopy using an adaptiva general linear model *NeuroImage* **46** 133–43

Akin A and Bunce S 2003 Quantifying brain hemodynamic response measured by functional optical imaging *Int. IEEE Engineering in Medicine and Biology Society (EMBS) Conf. on Neural Engineering* (Capri: IEEE) pp 503–6

Alaluf S, Atkins D, Barret K, Blount M, Carter N and Heath A 2002 Ethnic variation in melanin content and composition in photoexposed and photoprotected human skin *Pigment Cell Res.* **15** 112–8

Arridge S R, Hebden J C and Delpy D T 1997 Optical imaging in medicine: II. Modelling and reconstruction *Phys. Med. Biol.* **42** 841–53

Blasi A, Fox S, Everdell N, Volein A, Tucker L, Csibra G, Gibson A P, Hebden J C, Johnson M H and Elwell C E 2007 Investigation of depth dependent changes in cerebral haemodynamics during face perception in infants *Phys. Med. Biol.* **52** 6849–64

Boas D A, Chen K, Grebert D and Franceschini M A 2004 Improving the diffuse optical imaging spatial resolution of the cerebral hemodynamic response to brain activation in humans *Opt. Lett.* **29** 1506–8

Boas D A, Strangman G, Culver J P, Hoge R D, Jasdzewski G, Poldrack R A, Rosen B R and Mandeville J B 2003 Can the cerebral metabolic rate of oxygen be estimated with near-infrared spectroscopy? *Phys. Med. Biol.* **48** 2405–18

Bozkurt A, Rosen A, Rosen H and Onaral B 2005 A portable near infrared spectroscopy system for bedside monitoring of newborn brain *Biomed. Eng. Online* **4** 29

Cope M and Delpy D T 1988 System for long-term measurement of cerebral blood and tissue oxygenation on newborn infants by near infrared transillumination *Med. Biol. Eng. Comp.* **26** 289–94

Coyle S M, Ward T E, Markham C and McDarby G 2004 On the suitability of near-infrared (NIR) systems for next-generation brain-computer interfaces *Physiol. Meas.* **25** 815–22

Cui X, Bray S and Reiss A L 2010 Functional near infrared spectroscopy (NIRS) signal improvement based on negative correlation between oxygenated and deoxygenated hemoglobin dynamics *NeuroImage* **49** 3039–46

Custo A, Wells W M III, Barnett A H, Hillman E M C and Boas D A 2006 Effective scattering coefficient of the cerebral spinal fluid in adult head models for diffuse optical imaging *Appl. Opt.* **45** 4747–55

Dager S R and Friedman S D 2000 Brain imaging and the effects of caffeine and nicotine *Ann. Med.* **32** 592–9

Dehghani H, Srinivasan S, Pogue B W and Gibson A P 2009a Numerical modelling and image reconstruction in diffuse optical tomography *Phil. Trans. R. Soc.* A **367** 3073–93

Dehghani H, White B R, Zeff B W, Tizzard A and Culver J P 2009b Depth sensitivity and image reconstruction analysis of dense imaging arrays for mapping brain function with diffuse optical tomography *Appl. Opt.* **48** D137–43

Delpy D T, Cope M, Zee van der P, Arridge S R, Wray S and Wyatt J S 1988 Estimation of optical pathlength through tissue from direct time of flight measurement *Phys. Med. Biol.* **33** 1433–42

Devor A, Ulbert I, Dunn A K, Narayanan S N, Jones S R, Andermann M L, Boas D A and Dale A M 2005 Coupling of the cortical hemodynamic response to cortical and thalamic neuronal activity *Proc. Natl Acad. Sci.* **102** 3822–7

Diamond S G, Huppert T J, Kolehmainen V, Franceschini M A, Kaipio J P, Arridge S R and Boas D A 2006 Dynamic physiological modelling for functional diffuse optical tomography *NeuroImage* **30** 88–101

Diamond S G, Perdue K L and Boas D A 2009 A cerebrovascular response model for functional neuroimaging including dynamic cerebral autoregulation *Math. Biosci.* **220** 102–17

Duncan A, Meek J H, Clemence M, Elwell C E, Tyszczuk L, Cope M and Delpy D T 1995 Optical pathlength measurements on adult head, calf and forearm and the head of the newborn infant using phase resolved optical spectroscopy *Phys. Med. Biol.* **40** 295–304

Edwards A D 1995 Near infrared spectroscopy *Eur. J. Pediatr.* **154** S19–21

Elwell C E, Cope M, Edwards A D, Wyatt J S, Delpy D T and Reynolds E O R 1994 Quantification of adult cerebral hemodynamics by near-infrared spectroscopy *J. Appl. Physiol.* **77** 2753–60

Elwell C E, Springett R, Hillman E M C and Delpy D T 1999 Oscillations in cerebral haemodynamics—implications for functional activation studies *Adv. Exp. Med. Biol.* **471** 57–65

Essenpreis M, Elwell C E, Cope M, Zee van der P, Arridge S R and Delpy D T 1993 Spectral dependence of temporal point spread functions in human tissues *Appl. Opt.* **32** 418–25

Everdell N L, Gibson A P, Tullis I D C, Vaithianathan T, Hebden J C and Delpy D T 2005 A frequency multiplexed near-infrared topography system for imaging functional activation in the brain *Rev. Sci. Instrum.* **76** 093705

Franceschini M A and Boas D A 2004 Noninvasive measurement of neuronal activity with near-infrared optical imaging *NeuroImage* **21** 372–86

Franceschini M A, Joseph D K, Huppert T J, Diamond S G and Boas D A 2006 Diffuse optical imaging of the whole head *J. Biomed. Opt.* **11** 054007

Gibson A P and Dehghani H 2009 Diffuse optical imaging *Phil. Trans. R. Soc.* A **367** 3055–72

González-Alonso J, Dalsgaard M K, Osada T, Volianitis S, Dawson E A, Yoshiga C C and Secher N H 2004 Brain and central haemodynamics and oxygenation during maximal exercise in humans *J. Physiol.* **557** 331–42

Gratton G, Brumback C R, Gordon B A, Pearson M A, Low K A and Fabiani M 2006 Effects of measurement method, wavelength, and source–detector distance on the fast optical signal *NeuroImage* **32** 1576–90

Greisen G 2006 Is near-infrared spectroscopy living up to its promise? *Semin. Fetal Neonatal Med.* **11** 498–502

Haensse D, Szabo P, Brown D, Fauchère J-C, Niederer P, Bucher H-U and Wolf M 2005 New multichannel near-infrared spectrophotometry system for functional studies of the brain in adults and neonates *Opt. Express* **13** 4525–38

Hasan S, Pradervand S, Ahnaou A, Drinkenburg W, Tafti M and Franken P 2009 How to keep the brain awake? The complex molecular pharmacogenetics of wake promotion *Neuropsychopharmacology* **34** 1625–40

Hatakenaka M, Miyai I, Mihara M, Sakoda S and Kubota K 2007 Frontal regions involved in learning of motor skill—a functional NIRS study *NeuroImage* **34** 109–16

Hebden J C, Arridge S R and Delpy D T 1997 Optical imaging in medicine: I. Experimental techniques *Phys. Med. Biol.* **42** 825–40

Hebden J C, Gonzalez F M, Gibson A P, Hillman E M C, Yusof R M, Everdell N, Delpy D T, Zaccanti G and Martelli F 2003 Assessment of an *in-situ* temporal calibration method for time-resolved optical tomography *J. Biomed. Opt.* **8** 87–92

Heekeren H R, Obrig H, Wenzel R, Eberle K, Ruben J, Villringer K, Kurth R and Villringer A 1997 Cerebral haemoglobin oxygenation during sustained visual stimulation—a near-infrared spectroscopy study *Phil. Trans. R. Soc.* B **352** 743–50

Hemelt M W and Kang K 1999 Determination of a biological absorber depth utilizing multiple source–detector separations and multiple frequency values of near-infrared time-resolved spectroscopy *Biotechnol. Prog.* **15** 622–9

Herrmann M J, Walter A, Ehlis A C and Fallgatter A J 2006 Cerebral oxygenation changes in the prefrontal cortex: effects of age and gender *Neurobiol. Aging* **27** 888–94

Herrmann M J, Woidich E, Schreppel T, Pauli P and Fallgatter A J 2008 Brain activation for alertness measured with functional near-infrared spectroscopy (fNIRS) *Psychophysiology* **45** 480–6

Higashi T, Sone Y, Ogawa K, Kitamura Y T, Saiki K, Sagawa S, Yanagida T and Seiyama A 2004 Changes in regional cerebral blood volume in frontal cortex during mental work with and without caffeine intake: functional monitoring using near-infrared spectroscopy *J. Biomed. Opt.* **9** 788–93

Holper L, Biallas M and Wolf M 2009 Task complexity relates to activation of cortical motor areas during uni- and bimanual performance: a functional NIRS study *NeuroImage* **46** 1105–13

Hoshi Y 2007 Functional near-infrared spectroscopy: current status and future prospects *J. Biomed. Opt.* **12** 062106

Hoshi Y, Kobayashi N and Tamura M 2001 Interpretation of near-infrared spectroscopy signals: a study with a newly developed perfused rat brain model *J. Appl. Physiol.* **90** 1657–62

Hoshi Y, Shimada M, Sato C and Iguchi Y 2005 Reevaluation of near-infrared light propagation in the adult human head: implications for functional near-infrared spectroscopy *J. Biomed. Opt.* **10** 064032

Huppert T and Boas D A 2005 HomER: Hemodynamic Evoked Response NIRS data analysis GUI Photon Migration Imaging Lab, Massachusetts General Hospital/CNY, Charlestown, MA, USA http://www.nmr.mgh.harvard.edu/PMI/resources/homer/HomER_UsersGuide_05-07-28.pdf

Huppert T J, Diamond S G, Franceschini M A and Boas D A 2009 HomER: a review of time-series analysis methods for near-infrared spectroscopy of the brain *Appl. Opt.* **48** D280–98

IEC 2007 Safety of laser products *IEC 60825* International Electrotechnical Commission

Ito Y, Kennan R P, Watanabe E and Koizumi H 2000 Assessment of heating effects in skin during continuous wave infrared spectroscopy *J. Biomed. Opt.* **5** 383–90

Izzetoglu M, Chitrapu P, Bunce S and Onaral B 2010 Motion artefact cancellation in NIR spectroscopy using discrete Kalman filtering *Biomed. Eng. Online* **9** 16

Izzetoglu M, Devaraj A, Bunce S and Onaral B 2005 Motion artifact cancellation in NIR spectroscopy using wiener filtering *IEEE Trans. Biomed. Eng.* **52** 934–8

Jöbsis F F, Keizer J H, LaManna J C and Rosenthal M 1977 Reflectance spectrophotometry of cytochrome aa3 *in vivo J. Appl. Physiol.* **43** 858–72

Jurcak V, Tsuzuki D and Dan I 2007 10/20, 10/10 and 10/5 system revisited: their validity as a relative head-surface-based positioning systems *NeuroImage* **34** 1600–11

Kameyama M, Fukuda M, Uehara T and Mikuni M 2004 Sex and age dependencies of cerebral blood volume changes during cognitive activation: a multichannel near-infrared spectroscopy study *NeuroImage* **22** 1715–21

Katura T, Sato H, Fuchino Y, Yoshida T, Atsumori H, Kiguchi M, Maki A, Abe M and Tanaka N 2008 Extracting task-related activation components from optical topography measurement using independent component analysis *J. Biomed. Opt.* **13** 054008

Katura T, Tanaka N, Obata A, Sato H and Maki A 2006 Quantitative evaluation of interrelations between spontaneous low-frequency oscillations in cerebral hemodynamics and systemic cardiovascular dynamics *NeuroImage* **31** 1592–600

Koh P H, Glaser D E, Flandin G, Kiebel S J, Butterworth B, Maki A, Delpy D T and Elwell C E 2007 Functional optical signal analysis: a software tool for near-infrared spectroscopy data processing incorporating statistical parametric mapping *J. Biomed. Opt.* **12** 064010

Kohl M, Nolte C, Heekeren H R, Horst S, Scholz U, Obrig H and Villringer A 1998 Determination of the wavelength dependence of the differential pathlength factor from near-infrared pulse signals *Phys. Med. Biol.* **43** 1771–82

Kohno S 2007 Removal of the skin blood flow artifact in functional near-infrared spectroscopy imaging data through independent component analysis *J. Biomed. Opt.* **12** 062111

Koizumi H, Yamashita Y, Maki A, Yamamoto T, Ito Y, Itagaki H and Kennan R 1999 Higher-order brain function analysis by trans-cranial dynamic near-infrared spectroscopy imaging *J. Biomed. Opt.* **4** 403–13

Krekelberg B, Boynton G M and Wezel R J A v 2006 Adaptation: from single cells to BOLD signals *Trends Neurosci.* **29** 250–6

Kudo T, Mishima R, Yamamura K, Mostafeezur R, Zakir H M D, Kurose M and Yamada Y 2008 Difference in physiological responses to sound stimulation in subjects with and without fear of dental treatments *Odontology* **96** 44–9

Ladewig D, Dürsteler-MacFarland K M, Seifritz E, Hock C and Stohler R 2002 New aspects in the treatment of heroin dependence with special reference to neurobiological aspects *Eur. Psychiatry* **17** 163–6

Lee S-H 2004 Reducing the effects of ambient noise light in an indoor optical wireless system using polarizers *Microw. Opt. Technol. Lett.* **40** 228–31

Leff D R, Elwell C E, Orihuela-Espina F, Atallah L, Delpy D T, Darzi A W and Yang G-Z 2008a Changes in prefrontal cortical behaviour depend upon familiarity on a bimanual co-ordination task: an fNIRS study *NeuroImage* **39** 805–13

Leff D R, Orihuela-Espina F, Atallah L, Darzi A W and Yang G-Z 2007 Functional near infrared spectroscopy in novice and expert surgeons: a manifold embedding approach *Lecture Notes in Computer Science Medical Image Computing and Computer-Assisted Intervention (MICCAI'07) (Australia)* ed N Ayache *et al* pp 270–7

Leff D R, Orihuela-Espina F, Leong J J H, Atallah L, Darzi A W and Yang G-Z 2008b Modelling dynamic fronto-parietal behaviour durign minimally invasive surgery—a Markovian trip distribution approach *11th Int. Conf. on Medical Image Computing and Computer Assisted Intervention (MICCAI 2008) (New York, USA)* pp 270–7

Li C and Jiang H 2004 A calibration method in diffuse optical tomography *J. Opt. A: Pure Appl. Opt.* **6** 844–52

Lloyd-Fox S, Blasi A and Elwell C E 2009 Illuminating the developing brain: the past, present and future of functional near infrared spectroscopy *Neurosci. Biobehav. Rev.* **34** 269–84

Meek J H, Elwell C E, Khan M J, Romaya J, Wyatt J S, Delpy D T and Zeki S 1995 Regional changes in cerebral haemodynamics as a result of a visual stimulus measured by near infrared spectroscopy *Proc. R. Soc. Biol. Sci.* **261** 351–6

Mehagnoul-Schipper J, van der Kallen B F W, Colier W N J M, van der Sluijs M C, van Erning L J T O, Thijssen H O M, Oeseburg B, Hoefnagels W H L and Jansen R W M M 2002 Simultaneous measurements of cerebral oxygenation changes during brain activation by near-infrared spectroscopy and functional magnetic resonance imaging in healthy young and elderly subjects *Hum. Brain Mapp.* **16** 14–23

Morinaga K, Akiyoshi J, Matsushita H, Ichioka S, Tanaka Y, Tsuru J and Hanada H 2007 Anticipatory anxiety-induced changes in human lateral prefrontal cortex activity *Biol. Psychol.* **74** 34–8

Nakano T, Homae F, Watanabe H and Taga G 2008 Anticipatory cortical activation precedes auditory events in sleeping infants *Public Library of Science (PLoS) ONE J.* **3** e3912

Nakano T, Watanabe H, Homae F and Taga G 2009 Prefrontal cortical involvement in young infants' analysis of novelty *Cereb. Cortex* **19** 455–63

Obata A, Morimoto K, Sato H, Maki A and Koizumi H 2003 Acute effects of alcohol on haemodynamic changes during visual stimulation assessed using 24-channel near-infrared spectroscopy *Psychiatry Res.: Neuroimaging* **123** 145–52

Obrig H, Hirth C, Junge-Hülsing J G, Döge C, Wenzel R, Wolf T, Dirnagl U and Villringer A 1997 Length of resting period between stimulation cycles modulates hemodynamic response to a motor stimulus *Oxygen Transport to Tissue XVIII* ed E M Nemoto and J C LaManna (New York: Plenum) pp 471–80

Obrig H, Israel H, Kohl-Bareis M, Uludag K, Wenzel R, Müller B, Arnold G and Villringer A 2002 Habituation of the visually evoked potential and its vascular response: implications for neurovascular coupling in the adult head *NeuroImage* **17** 1–18

Obrig H, Neufang M, Wenzel R, Kohl M, Steinbrink J, Einhäupl K and Villringer A 2000 Spontaneous low frequency oscillations of cerebral hemodynamics and metabolism in human adults *NeuroImage* **12** 623–39

Okada E and Delpy D T 2003a Near-infrared light propagation in an adult head model: I. Modeling of low level scattering in the cerebrospinal fluid layer *Appl. Opt.* **42** 2906–14

Okada E and Delpy D T 2003b Near-infrared light propagation in an adult head model: II. Effect of superficial tissue thickness on the sensitivity of the near-infrared spectroscopy signal *Appl. Opt.* **42** 2915–22

Okamoto M *et al* 2004 Three-dimensional probabilistic anatomical cranio–cerebral correlation via the international 10–20 system oriented for transcranial functional brain mapping *NeuroImage* **21** 99–111

Oldfield R C 1970 The assessment and analysis of handedness: the Edinburgh inventory *Neuropsychologia* **9** 97–113

Orihuela-Espina F, Leff D R, James D R C, Darzi A W and Yang G-Z 2008 *Data Integrity in Continuous Wave Functional Near Infrared Spectroscopy Neuroimaging* (London: Imperial College London) p 42

Orihuela-Espina F, Leff D R, James D R C, Darzi A W and Yang G-Z 2009 ICNA: a software tool for manifold embedded based analysis of functional near infrared spectroscopy data *Annu. Meeting of the Organization of Human Brain Mapping (OHBM 2009) (San Francisco, CA, USA) NeuroImage* **47** S59

Ottevanger P B, Therasse P, Velde C v d, Bernier J, Krieken H v, Grol R and Mulder P D 2003 Quality assurance in clinical trials *Crit. Rev. Oncol./Hematol.* **47** 213–35

Peña M, Maki A, Kovačić D, Dehaene-Lambertz G, Koizumi H, Bouquet F and Mehler J 2003 Sounds and silence: an optical topography study of language recognition at birth *Proc. Natl Acad. .Sci.* **100** 11702–5

Petersson K M, Nichols T E, Poline J-B and Holmes A P 1999a Statistical limitations in functional neuroimaging: I. Non-inferential methods and statistical models *Phil. Trans. R. Soc.* B **354** 1239–60

Petersson K M, Nichols T E, Poline J-B and Holmes A P 1999b Statistical limitations in functional neuroimaging: II. Signal detection and statistical inference *Phil. Trans. R. Soc* B **354** 1261–81

Pieniążek W, Dimitrow P P and Jasiński T 2001 Comparison of the effect of perindopril and acebutolol on cerebral hemodynamics in hypertensive patients *Cardiovasc. Drugs Ther.* **15** 63–7

Plichta M M, Heinzel S, Ehlis A C, Pauli P and Fallgatter A J 2007a Model-based analysis of rapid event-related functional near-infrared spectroscopy (NIRS) data: a parametric validation study *NeuroImage* **35** 625–34

Plichta M M, Herrmann M J, Baehne C G, Ehlis A C, Richter M M, Pauli P and Fallgatter A J 2006 Event-related functional near-infrared spectroscopy (fNIRS): are the measurements reliable? *NeuroImage* **31** 116–24

Plichta M M, Herrmann M J, Baehne C G, Ehlis A C, Richter M M, Pauli P and Fallgatter A J 2007b Event-related functional near-infrared spectroscopy (fNIRS) based on craniocerebral correlations: reproducibility of activation? *Hum. Brain Mapp.* **28** 733–41

Robertson F C, Douglas T S and Meintjes E M 2010 Motion artefact removal for functional near infrared spectroscopy: a comparison of methods *IEEE Trans. Biomed. Eng.* **57** 1377–87

Rolfe P 2000 *In vivo* near infrared spectroscopy *Annu. Rev. Biomed. Eng.* **2** 715–54

Saager R and Berger A 2008 Measurement of layer-like hemodynamic trends in scalp and cortex: implications for physiological baseline suppression in functional near-infrared spectroscopy *J. Biomed. Opt.* **13** 034017

Sato H, Kiguchi M, Kawaguchi F and Maki A 2004 Practicality of wavelength selection to improve signal-to-noise ratio in near-infrared spectroscopy *NeuroImage* **21** 1554–62

Sato H, Kiguchi M and Maki A 2006a Wavelength dependence of effective pathlength factor in noninvasive optical measurements of human brain functions *Japan. J. Appl. Phys.* **45** L361–L3

Sato H, Kiguchi M, Maki A, Fuchino Y, Obata A, Yoro T and Koizumi H 2006b Within-subject reproductibility of near-infrared spectroscopy signals in sensorimotor activation after 6 months *J. Biomed. Opt.* **11** 014021

Sato H, Tanaka N, Uchida M, Hirabayashi Y, Kanai M, Ashida T, Konishi I and Maki A 2006c Wavelet analysis for detecting body movement artifacts in optical topography signals *NeuroImage* **33** 580–7

Sato T, Ito M, Suto T, Kameyama M, Suda M, Yamagishi Y, Ohshima A, Uehara T, Fukuda M and Mikuni M 2007 Time courses of brain activation and their implications for function: a multichannel near-infrared spectroscopy study during finger tapping *Neurosci. Res.* **58** 294–304

Schmidt F E W, Fry M E, Hillman E M C, Hebden J C and Delpy D T 2000 A 32-channel time-resolved instrument for medical optical tomography *Rev. Sci. Instrum.* **71** 256–65

Schroeter M L, Zysset S, Kruggel F and von Crammon D Y 2003 Age dependency of the haemodynamic response as measured by functional near-infrared spectroscopy *NeuroImage* **19** 555–64

Sheth S A, Nemoto M, Guiou M W, Walker M A, Pouratian N and Toga A W 2004 Linear and nonlinear relationships between neuronal activity, oxygen metabolism and hemodynamic responses *Neuron* **42** 347–55

Siegel A M, Marota J J A and Boas D A 1999 Design and evaluation of a continuous-wave diffuse optical tomography system *Opt. Express* **4** 287–98

Singh A K, Okamoto M, Dan H, Jurcak V and Dan I 2005 Spatial registration of multi-channel fNIRS data to MNI space without MRI *NeuroImage* **27** 842–51

Stott J J, Culver J P, Arridge S R and Boas D A 2003 Optode positional calibration in diffuse optical tomography *Appl. Opt.* **42** 3154–62

Strangman G, Boas D A and Sutton J P 2002 Non-invasive neuroimaging using near-infrared light *Biol. Psychiatry* **52** 679–93

Strangman G, Franceschini M A and Boas D A 2003 Factors affecting the accuracy of near-infrared spectroscopy concentration calculations for focal changes in oxygenation parameters *NeuroImage* **18** 865–79

Suda M, Fukuda M, Sato T, Iwata S, Song M, Kameyama M and Mikuni M 2009 Subjective feeling of psychological fatigue is related to decreased reactivity in ventrolateral prefrontal cortex *Brain Res.* **1252** 152–60

Suzuki M, Miyai I, Ono T, Oda I, Konishi I, Kochiyama T and Kubota K 2004 Prefrontal and premotor cortices are involved in adapting walking and running speed on the treadmill: an optical imaging study *NeuroImage* **23** 1020–6

Svasaand L O and Elligsen R 1983 Optical properties of the human brain *Photochem. Photobiol.* **38** 293–9

Tachtsidis I, Leung T S, Chopra A, Koh P H, Reid C B and Elwell C E 2009 False positives in functional near infrared topography *Adv. Exp. Med. Biol.* **645** 307–14

Taga G, Asakawa K, Maki A, Konishi Y and Koizumi H 2003 Brain imaging in awake infants by near-infrared optical topography *Proc. Natl Acad. Sci.* **100** 10722–7

Takahashi K *et al* 2000 Activation of the visual cortex imaged by 24 channel near-infrared spectroscopy *J. Biomed. Opt.* **5** 93–6

Tanida M, Katsuyama M and Sakatani K 2007 Relation between mental stress-induced prefrontal cortex activity and skin conditions: a near-infrared spectroscopy study *Brain Res.* **1184** 210–6

Thilwind R E, Hooft G t and Uzunbajakava N E 2009 Improved depth resolution in near-infrared diffuse reflectance spectroscopy using obliquely oriented fibers *J. Biomed. Opt.* **14** 024026

Toronov V, Franceschini M A, Filiaci M, Fantini S, Wolf M, Michalos A and Gratton E 2000 Near-infrared study of fluctuations in cerebral hemodynamics during rest and motor stimulation: temporal analysis and spatial mapping *Med. Phys.* **27** 801–15

Tsuzuki D, Jurcak V, Singh A K, Okamoto M, Watanabe E and Dan I 2007 Virtual spatial registration of stand-alone fNIRS data to MNI space *NeuroImage* **34** 1506–18

Uludag K, Kohl M, Steinbrink J, Obrig H and Villringer A 2002 Cross talk in the Lambert–Beer calculation for near-infrared wavelengths estimated by Monte Carlo simulations *J. Biomed. Opt.* **7** 51–9

Uludag K, Steinbrink J, Villringer A and Obrig H 2004 Separability and cross-talk: optimizing dual wavelength combinations for near-infrared spectroscopy of the adult head *NeuroImage* **22** 583–9

Villringer A and Chance B 1997 Non-invasive optical spectroscopy and imaging of human brain function *Trends Neurosci.* **20** 435–42

Virtainen J, Noponen T and Meriläinen P 2009 Comparison of principal and independent component analysis in removing extracerebral interference from near-infrared spectroscopy signals *J. Biomed. Opt.* **14** 054032

Watanabe E, Yamashita Y, Maki A, Ito Y and Koizumi H 1996 Non-invasive functional mapping with multi-channel near infra-red spectroscopy topography in humans *Neurosci. Lett.* **205** 41–4

Watanabe H, Homae F, Nakano T and Taga G 2008 Functional activation in diverse regions of the developing brain of human infants *NeuroImage* **43** 346–57

White B R, Snyder A Z, Cohen A L, Petersen S E, Raichle M E, Schlaggar B L and Culver J P 2009 Resting-state functional connectivity in the human brain revealed with diffuse optical tomography *NeuroImage* **47** 148–56

Wilcox T, Bortfield H, Woods R and Wruck E 2005 Using near-infrared spectroscopy to assess neural activation during object processing in infants *J. Biomed. Opt.* **10** 011010

Williams J 2001 Controlling the temperature of fiber-optic lasers *EDN Magazine* 5th July pp 99–108

Wyatt J S, Cope M, Delpy D T, Richardson C E, Edwards A D, Wray S and Reynolds E O R 1990 Quantitation of cerebral blood volume in human infants by near-infrared spectroscopy *J. Appl. Physiol.* **68** 1086–91

Yamamoto T, Maki A, Kadoya T, Tanikawa Y, Yamada Y, Okada E and Koizumi H 2002 Arranging optical fibers for the spatial resolution improvement of topographical images *Phys. Med. Biol.* **47** 3429–40

Yamashita Y, Maki A and Koizumi H 2001 Wavelength dependence of the precision of non-invasive optical measurement of oxy-, deoxy- and total-hemoglobin concentration *Med. Phys.* **28** 1108–14

Yamashita Y, Maki A, Watanabe E, Koizumi H and Kawaguchi F 1998 Development of optical topography for noninvasive measurement of human brain activity *Medix* **29** (August) http://www.hitachi-medical.co.jp/medix/pdf/vol29/29_06e.pdf

Ye J C, Tak S, Jang K E, Jung J and Jang J 2009 NIRS-SPM: Statistical parametric mapping for near-infrared spectroscopy *NeuroImage* **44** 428–47

Zee van der P *et al* 1992 Experimentally measured optical pathlength for the adult head, calf and forearm and the head of the newborn infant as a function of inter optode spacing *Adv. Exp. Med. Biol.* **316** 143–53

Zhang Y, Brooks D H and Boas D A 2005a A haemodynamic response function model in spatio-temporal diffuse optical tomography *Phys. Med. Biol.* **50** 4625–44

Zhang Y, Brooks D H, Franceschini M A and Boas D A 2005b Eigenvector-based spatial filtering for reduction of physiological interference in diffuse optical imaging *J. Biomed. Opt.* **10** 011014